Supporting Information

New insights into cis-autoproteolysis reveal a reactive state formed through conformational rearrangement

Andrew R Buller, Michael F Freeman, Nathan T Wright, Joel F Schildbach, Craig A Townsend

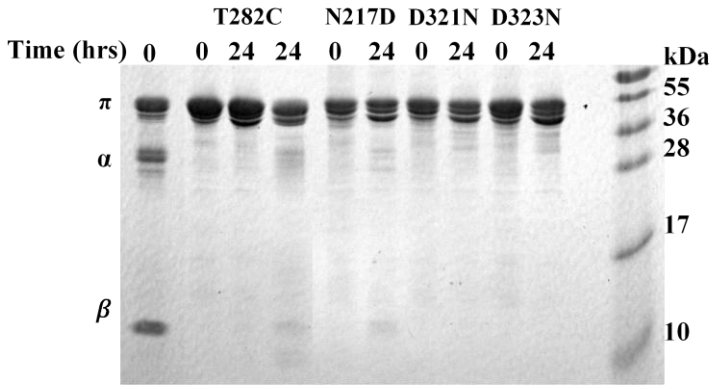

Fig. S1. Mutational disruption of autoproteolysis. Samples run on 15% SDS-PAGE. Lane1: wt-ThnT, showing the uncleaved (π) band and the two cleavage products (α,β); Lane 2-3: T282C; lane 4: T282C + 500mM NH_2OH; lane 5-6: N217D; lane 7-8: D321N; lane 9-10: D323N; lane 11: Fermentas Pre-stained Protein Ladder (relevant molecular weights on figure).

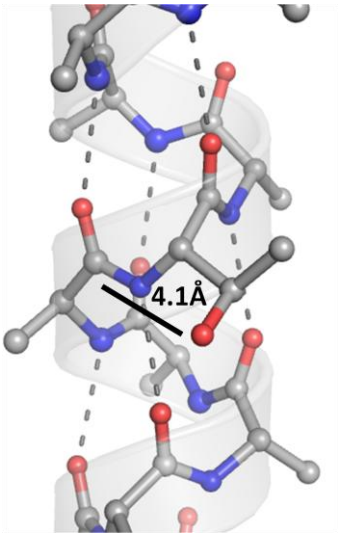

Fig. S2. A threonine residue on a generic α-helix. The long distance between the reactive atoms and inappropriate geometry readily account for the inability of α-helices to support *cis*-autoproteolysis without disrupting the hydrogen bond network (grey dashes) of the helix.

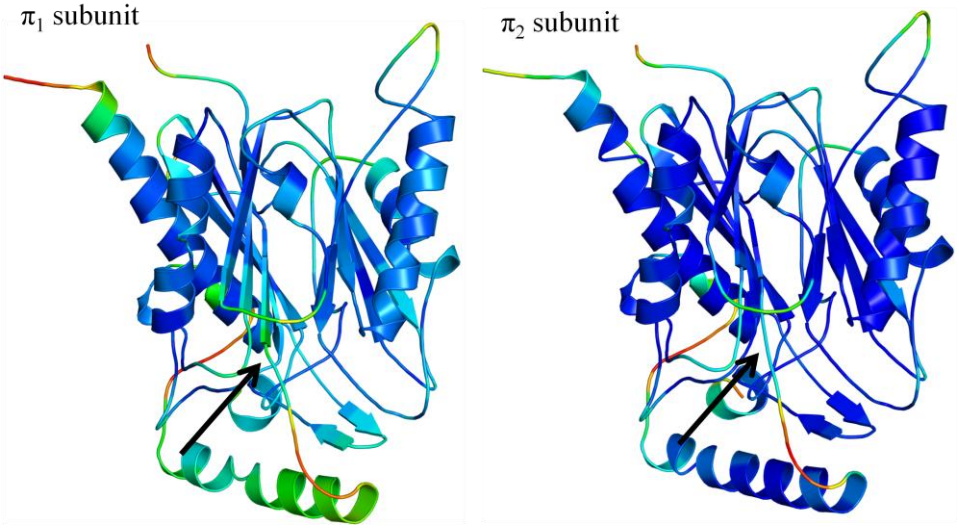

Fig. S3. Ribbon diagram of T282C colored by B-factor of Cα from low (blue) to high (red) shows the average thermal motion of the π_2 subunit is significantly lower than that of the π_1 subunit. The loop leading into the scissile bond (black arrow) is moderately disordered, consistent with its high B-factors and dissociation after autoproteolysis.

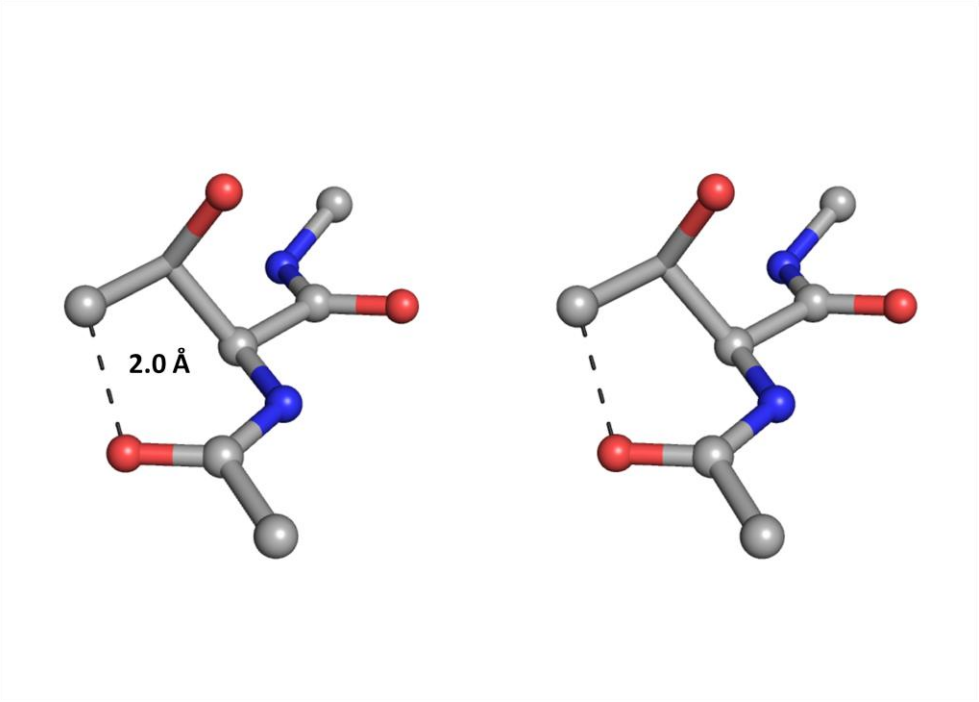

Fig. S4. Stereo view of the reactive rotamer for state B of ThnT. This gives rise to a strong steric clash that prevents formation of this rotamer, precluding autoproteolysis. The backbone angles shown here are similar to those found in the structures of several other Thr-utilizing Ntn hydrolases (PDB ID: 2LJQ, 2E0W and 3C17, see Table S1), suggesting they too represent inactive states.

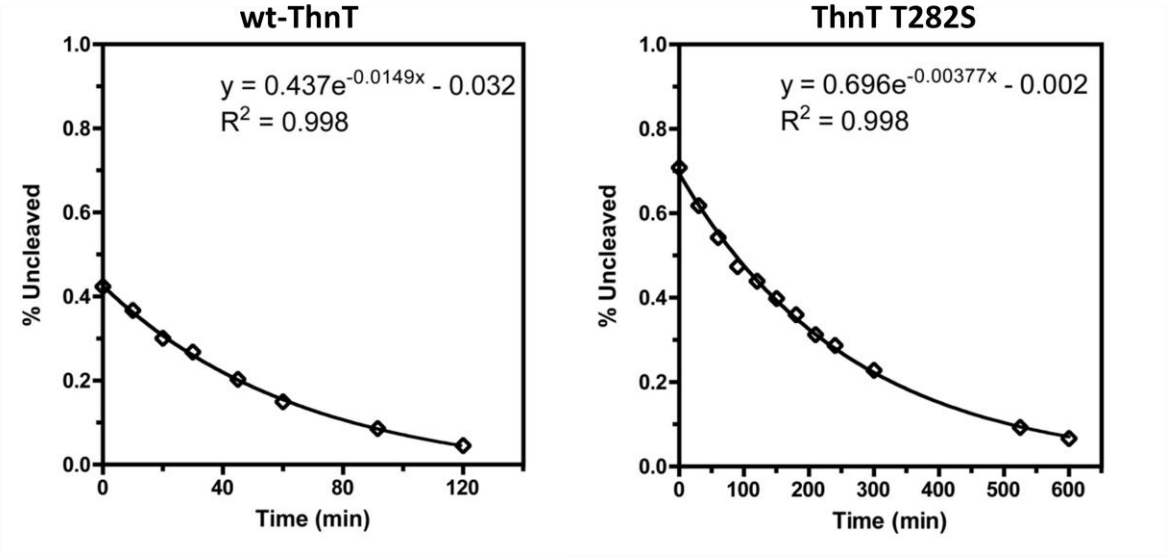

Fig. S5. Representative fits for kinetic analysis of autoproteolysis. Data were derived from densitometry measurements, as described in Materials and Methods. From three independent measurements $k_{autoproteolysis}$ for wt-ThnT was determined to be $k = 0.015 \pm 0.002$ min^{-1}; for ThnT T282S, $k = 0.00378 \pm 0.0002$ min^{-1}.

Table S1. Active site geometries of precursor *cis*-autoproteolytic proteins

					Geometry of Nucleophile							
Enzyme	**Organism**	**Nucleophile**	**Variant**	**PDB**	**Phi**	**Psi**	**Omega**	**Bin***	**RR†**	**P(RR) ‡**	**RRE §**	**Ref**
ThnT (State A)	Streptomyces cattleya	Thr	T282C	3S3U	87	114	177	(90,110)	*g*-	0.632	1.6	
Proteasome (beta subunit)	Thermoplasma acidophilum	Thr	T1A	----	75	158	177	(80,160)	*g*-	0.08	0.6	7
ThnT (State B)	Streptomyces cattleya	Thr	T282C	3S3U	-175	170	159	(-170,170)	*g*+	<0.001		
Glycosylasparaginase	Elizabethkingia meningoseptica	Thr	T152C	2LJQ	-175	166	161	(-170,170)	*g*+	<0.001		34
Glycosylasparaginase	Elizabethkingia meningoseptica	Thr	W11F	9GAF	-150	146	160	(-150, 150)	*g*-	0.076	0.8	19
Glycosylasparaginase	Elizabethkingia meningoseptica	Thr	T152A	9GAA	-69	160	-167	(-70, 160)	N/A	N/A		34
γ-Glutamyltranspeptidase	Escherichia coli	Thr	T391A	2E0W	176	180	175	(180,180)	*g*+	<0.001		39
L-Asparaginase EcAIII	Escherichia coli	Thr	T178A	3C17	-176	176	178	(-180, 180)	*g*+	<0.001		40
L-Asparaginase EcAIII	Escherichia coli	Thr	T178A	2ZAK	-82	179	-174	(-80, 180)	N/A	N/A		41
Taspase1	Homo sapiens	Thr	D233A	2A8I	-80	173	179	(-80, 170)	N/A	N/A		24
Glutaryl 7-aminocephalosporanic Acid Acylase	*Pseudomonas* sp. strain GK16	Ser	S170A	1OQZ	-176	162	175	(180,160)	*g*+	0.729		29
Cephalosporin Acylase	Pseudomonas diminuta	Ser	S170A	1KEH	-174	170	178	(-170,170)	*g*+	0.884		28
Penicillin V Acylase	Bacillus sphaericus	Cys	C4S	2IWM	166	161	172	(170,160)	*g*+	0.805		N/A
Isopenicillin N Acylase	Penicillium chyrsogenum	Cys	C103A	2X1C	-169	155	168	(-170,160)	*g*+	0.855		35

* Rounded (phi, psi) angles from the geometry found in the X-ray crystal structure

† RR = Reactive rotamer, determined by ability to satisfy B-D trajectory, allowing for minor conformational changes.

‡ Probability of forming RR determined from backbone-dependent rotamer distributions in (29) using a 5% smoothing library.

§ RRE estimated by the ratio P(RR,Thr)/P(RR, Ser). Value only displayed if both terms are >0.001 and Thr is the wild-type nucleophile. This value

Table S2. Data collection, MAD and refinement statistics

Modification	native		ethyl mercury phosphate	
Space group	$P2_12_12$		$P2_12_12$	
Cell dimensions (Å)	a,b,c = 140.5, 68.7, 73.8		a,b,c = 140.6, 69.0, 73.8	
Data Processing				
Wavelength (Å)	0.8001	1.0036	0.7336	1.1010
Resolution (Å)	50 - 1.60	50 - 1.65	50 - 1.9	50 - 1.77
Last Bin	1.65 - 1.60	1.70-1.65	1.97-1.9	1.86-1.77
No. Observations	606,444	520,220	447,896	503,903
Completeness (%)	94.5 (68.3)	94.1 (54.8)	100 (100)	99.3 (93.4)
R_{merge} (%)	5.8 (66.4)	4.8 (34.8)	6.0 (51.1)	4.4 (45.9)
I/σI	31.1 (1.2)	34.2(2.2)	36.4 (4.62)	50.0 (3.7)
Redundancy	6.8 (3.7)	6.8 (3.3)	7.5 (7.4)	7.2 (5.5)
Refinement				
Total no. of reflections	84968			
Total no. of atoms	5923			
No. of waters	713			
FOM	0.881			
R_{work} (%)	15.8 (33.6)			
R_{free} (%)	19.1 (36.3)			
Ramachandran plot allowed, %	99.8			
Favored, %	98.6			
Outliers, %	0.2			

Values in parenthesis are for the highest resolution shell (1.65 - 1.60 Å)

R_{merge} is $\Sigma|Io - I| / \Sigma Io$, where Io is the intensity of an individual reflection, and I is the mean intensity for multiply recorded reflections

R_{work} is $||Fo - Fc|| / Fo$, where Fo is an observed amplitude and Fc a calculated amplitude;

R_{free} is the same statistic calculated over a 5% subset of the data that has not been included during refinement.